Original Article
J Vet Sci 2015, 16(3), 307-315 · http://dx.doi.org/10.4142/jvs.2015.16.3.307

Quantitative determination of 12-hydroxyeicosatetraenoic acids by chiral liquid chromatography tandem mass spectrometry in a murine atopic dermatitis model

Seong-Ho Hong[1,†], Ji Eun Han[2,†], Ji-Seung Ko[3], Sun Hee Do[3], Eung Ho Lee[1,*], Myung-Haing Cho[1,4,5,6,7,*]

[1]*Laboratory of Toxicology, BK21 PLUS Program for Creative Veterinary Science Research, Research Institute for Veterinary Science and College of Veterinary Medicine, Seoul National University, Seoul 151-742, Korea*
[2]*Chemical and Material Components Center, Korea Testing Certification (KTC), Gunpo 435-823, Korea*
[3]*Department of Clinical Pathology, College of Veterinary Medicine, Konkuk University, Seoul 143-701, Korea*
[4]*Graduate School of Convergence Science and Technology, and* [6]*Advanced Institute of Convergence Technology, Seoul National University, Suwon 443-270, Korea*
[5]*Graduate Group of Tumor Biology, Seoul National University, Seoul 151-742, Korea*
[7]*Institute of Green Bio Science Technology, Seoul National University, Pyeongchang 232-916, Korea*

Atopic dermatitis, one of the most important skin diseases, is characterized by both skin barrier impairment and immunological abnormalities. Although several studies have demonstrated the significant relationship between atopic dermatitis and immunological abnormalities, the role of hydroxyeicosatetraenoic acids (HETE) in atopic dermatitis remains unknown. To develop chiral methods for characterization of 12-HETE enantiomers in a 1-chloro-2,4-dinitrochlorobenzene (DNCB)-induced atopic dermatitis mouse model and evaluate the effects of 12-HETE on atopic dermatitis, BALB/c mice were treated with either DNCB or acetone/olive oil (AOO) to induce atopic dermatitis, after which 12(R)- and 12(S)-HETEs in the plasma, skin, spleen, and lymph nodes were quantified by chiral liquid chromatography-tandem mass spectrometry. 12(R)- and 12(S)-HETEs in biological samples of DNCB-induced atopic dermatitis mice increased significantly compared with the AOO group, reflecting the involvement of 12(R)- and 12(S)-HETEs in atopic dermatitis. These findings indicate that 12(R)- and 12(S)-HETEs could be a useful guide for understanding the pathogenesis of atopic dermatitis.

Keywords: (±)12-hydroxyeicosatetraenoic acid, arachidonic acid, atopic dermatitis, chiral liquid chromatography tandem mass spectrometry

Introduction

Eicosanoids are signaling molecules produced by the oxygenation of arachidonic acid that are synthesized by all cutaneous cell types and involved in inflammatory responses associated with allergy, injury, and acute or chronic skin disease [13]. Over 100 different eicosanoids with potent bioactive signaling capacity have been identified to date. Several classes of eicosanoids exist, including prostaglandins, prostacyclins, thromboxanes, leukotrienes, epoxyeicosatrienoic acids, hydroxyeicosatetraenoic acids (HETE), hydroperoxyeicosatetraenoic acids (HpETEs), and lipoxins [7].

Recent studies have indicated that 12 lipoxygenases (Lox), which are enantiomer enzymes catalyzing the conversion of arachidonic acid to 12-HpETEs (the precursors to 12-HETEs), play a crucial role in skin barrier dysfunction and induce skin diseases [6,19]. Abstracting hydrogen from C-10 of arachidonic acid is the first reaction in the 12 Lox pathway. This reaction results in the formation of an arachidonic acid radical that reacts with oxygen to generate 12-HpETE. The 12-HETE is then catalyzed by glutathione peroxidase (GPx), after which glutathione (GSH) is oxidized to glutathione disulfide (panel A in Fig. 1) [18].

The lipoxygenase family has been identified by molecular cloning (Table 1). Mammalian lipoxygenase cDNAs that generate

Received 19 Jan. 2015, Revised 24 Feb. 2015, Accepted 7 Mar. 2015
*Corresponding authors: Tel: +82-2-880-1276; Fax: +82-2-873-1268; E-mails: dmdgh82@naver.com (EH Lee), mchotox@snu.ac.kr (MH Cho)
†The first two authors contributed equally to this work.
pISSN 1229-845X
eISSN 1976-555X

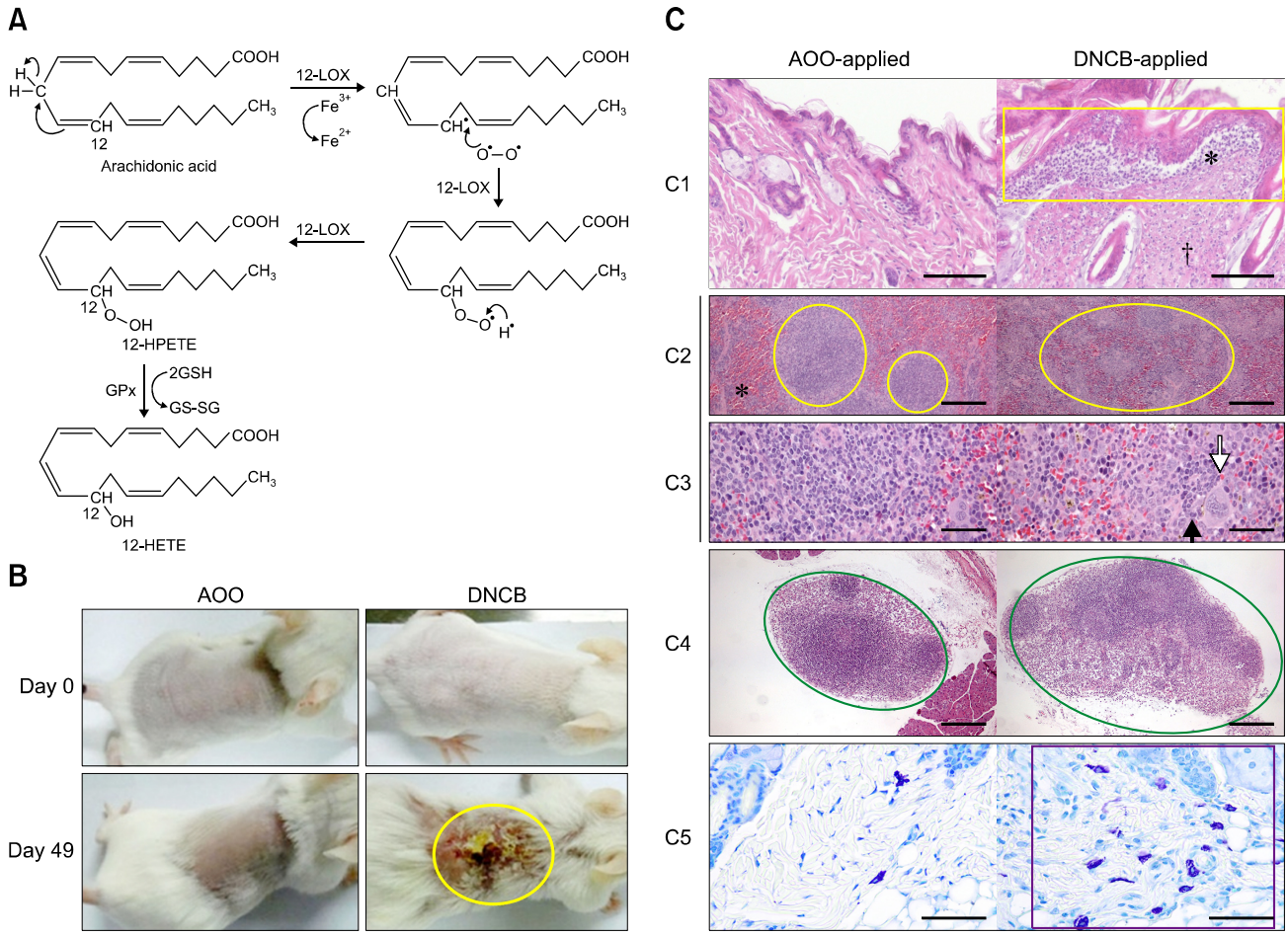

Fig. 1. (A) Mechanism of 12 lipoxygenase (Lox) catalyzed arachidonic acid transformation and comparison of (B) skin manifestations and (C) histopathology in acetone/olive oil (AOO) or 1-chloro-2,4-dinitrochlorobenzene (DNCB)-treated mice. (A) Hydrogen is abstracted from the bisallylic methylene. Re-arrangement of radicals causes the formation of a cis-trans conjugated diene system. The molecular dioxygen is inserted sterospecifically, forming a peroxy-radical. This substance is subsequently reduced to a hydroperoxide anion. 12- hydroxyeicosatetraenoic acid (HETE) is catalyzed by glutathione peroxidase (GPx), and glutathione (GSH) is oxidized to glutathione disulfide [17]. (B) The upper row photos were taken before treatment with AOO and DNCB. No skin lesions were detected in AOO-treated mice at 49 days. Erythema, scaling, and hemorrhagic crust (yellow circle) were observed in DNCB-treated mice at 49 days. These animals were treated by application of 100 μL of 1% DNCB in AOO onto the shaved back skin at 1, 4, and 7 weeks to induce atopic dermatitis. (C) Hematoxylin and eosin (H&E) staining of dorsal skin lesions (C1), spleen (C2 and 3), lymph nodes (C4) and toluidine blue staining of dorsal skin lesions (C5) in AOO or DNCB-treated mice. (C1) H&E staining of DNCB-treated dorsal skin lesions revealed hyperkeratosis, superficial pyoderma, and infiltration of inflammatory cells (box). *Epidermis. †Dermis. (C2) DNCB-treated mice spleen showed heterogeneous and indistinct white pulp (circle). *Red pulp. (C3) The number of reticular (black arrow) and giant cells (white arrow) increased in DNCB-treated mice compared with AOO-treated mice. (C4) H&E staining of lymph nodes in DNCB-treated mice showed mild lymphocyte depletion and granular lymphocytes (circle) compared with those in AOO-treated mice. (C5) Higher magnification of subcutaneous fatty layer in the DNCB-treated dorsal skin lesion showed massive infiltration of mast cells (box) under toluidine blue. Scale bars = 100 μm (C1), 200 μm (C2 and 4), 50 μm (C3 and 5).

12(R)-HETE have been cloned, but the cDNA have yet to be investigated in detail [11].

12-HETEs in human skin was first reported in 1975 [8], when the involved areas of epidermis in psoriasis were found to have markedly increased concentrations of free arachidonic acid and 12-HETEs. Many chiral polyunsaturated hydroxyl fatty acids are generated by enzymatic metabolism of arachidonic, linoleic, and 11, 14-eicosadienoic acid, which have been identified in inflamed skin scales. Inflamed skin scales contain 9-HODE, 13-HODE, 5-HETE, 8-HETE, 9-HETE, 11-HETE, 12-HETE, 15-HETE and 15 hydroxyeicosadienoic acid (15-HEDE). Among these derivatives, 12-HETE is the most abundant [1]. Atopic dermatitis (AD) is a chronic inflammatory, relapsing, non-contagious, and pruritic skin disorder. AD is a major skin

disease worldwide, occurring at rates of 20% in children and occasionally persisting into adulthood [3,17]. AD is caused by both skin barrier dysfunction and immunological abnormalities. This condition is frequently associated with elevated serum levels of IgE antibody and a T-cell (Th2)-dominant immune response [16].

We hypothesized that a significant relationship exists between AD and (±)12-HETEs, and the levels of (±)12-HETEs are changed in inflammatory biological samples. Therefore, we investigated the (±)12-HETEs levels in biological samples of a 1-chloro-2,4-dinitrochlorobenzene (DNCB)-induced AD murine model by chiral liquid chromatography-tandem mass spectrometry (LC-MS/MS) to identify a novel and useful AD biomarker.

Materials and Methods

Chemical and reagents

DNCB (99% purity) was purchased from Kanto Chemical (Japan). A mouse IgE enzyme-linked immunosorbent assay (ELISA) kit was purchased from Shibayagi (Japan). LC standards of 12(R)-HETE, 12(S)-HETE, (±)12-HETEs, and 12(S)-HETE-d_8 were purchased from Cayman Chemical (USA) and stored at −20°C until use. High performance liquid chromatography grade glacial acetic acid and all other chemicals were purchased from J.T.Baker (USA).

Table 1. Murine lipoxygenases

Lipoxygenase	Gene name
5-lipoxygenase (5-LO, 5-LOX)	*Alox5*
8-lipoxygenase (8-LO, 8-LOX)	*Alox8*
Platelet-type 12-lipoxygenase (P-12LO, 12-LOX)	*Alox12*
Leukocyte-type 12-lipoxygenase (L-12LO, 12/15LO, 12/15-LOX)	*Alox15*
Epidermal-type 12-lipoxygenase (e-12LO, e-LOX-1)	*Aloxe*
12(R)-lipoxygenase (12(R)-LO, e-LOX-2)	*Alox12b*
Epidermis-type lipoxygenase-3 (e-LOX-3)	*Aloxe3*

DNCB-induced AD

Eight week-old female BALB/c mice were obtained from Koatech (Korea). The mice were allowed to acclimatize for 5 days before use in experiments. Animals were housed in groups of five in cages identified by a card indicating the test number, animal number, test article, and duration. Animals were kept at room temperature (22°C) and a humidity of 50% under a 12 h light/12 h dark cycle, and were monitored daily during the experiment. Throughout the experimental period, animals were allowed free access to food and water.

The animals were treated by application of 100 μL 1% DNCB in acetone/olive oil (AOO) onto the shaved back skin at 1, 4, and 7 weeks to induce AD. Control animals were treated with AOO alone at the same times [8]. The body weight of DNCB or AOO-treated mice was measured at day 0 and day 49 (Table 2). All animal experimental protocols were approved by the Seoul National University Institutional Animal Care and Use Committee (SNU-120628-2).

Measurement of total IgE in serum

Serum samples were obtained by centrifugation (1,700 × g, 10 min) of blood collected on day 49 after three DNCB and AOO applications. Total IgE concentration was measured using a mouse IgE ELISA kit (Shibayagi, Japan) according to the manufacturer's instructions.

Histopathology

At termination of the *in vivo* study period, all animals were euthanized and examined. Skin, spleen, and lymph nodes were fixed in 10% neutral buffered formalin after necropsy, embedded in paraffin, and sectioned into 4 μm slices. Pathological changes were evaluated and compared between groups. Selected sections were stained with hematoxylin and eosin (H&E) and toluidine blue for mast cell infiltration.

Sample preparation for LC-MS/MS analysis

Sections of mouse skin (~1.5 cm × 1.5 cm, ~0.7 g), spleen, and lymph nodes were immersed in liquid nitrogen for 1 second, then homogenized. All lipids were extracted using the Bligh and Dyer method [2]. Samples containing 1 mL NaCl were

Table 2. Body weight (g) of DNCB and AOO-treated mice

	DNCB		AOO	
	Day 0	Day 49	Day 0	Day 49
Mouse 1	17.02	22.11	18.75	24.11
Mouse 2	17.71	22.80	17.91	23.01
Mouse 3	18.02	23.30	18.82	22.88
Mouse 4	17.58	22.88	18.36	22.13
Mouse 5	17.41	24.18	17.97	23.13

homogenized in a mixture of chloroform: methanol (1 : 2, v/v) and vortexed for 10 to 15 min. Next, 1.25 mL chloroform was added and mixed for 1 min, after which 1.25 mL NaCl was added and mixed for an additional 1 min before centrifugation (1,609 × g, 15 min). The upper phase was discarded, and the lower phase was collected through a 0.45 μm syringe filter (13 mm cellulose acetate; Advantec, USA) and then evaporated in a vacuum rotary evaporator.

The residue was reconstituted in 1,000 μL of mobile phase, sonicated, and stored at −20°C until LC-MS/MS analysis. For analysis, sample was transferred to an autosampler vial, after which 30 μL was injected. Additionally, an internal standard (I.S.) [12(S)-HETE-d_8] was prepared in 400 ng/mL methanol and added to all composite standards to give a final concentration of 100 ng/mL. The peak-area ratios of compound to 12(S)-HETE-d_8 were calculated and plotted against the concentrations of the calibration standards.

Apparatus and chiral analysis of HETEs

Chiral separation was performed on an Agilent 6430 triple quad LC/MS system with electrospray ionization (ESI) and negative ion detection (Agilent Technologies, USA). The (±)12-HETEs were separated using a ChiralPak AD-RH column (150 × 4.6 mm, 5 μm particle size; Daicel Corporation, France) and isocratic elution with methanol: water: acetic acid (95 : 5 : 0.1, v/v). The system flow rate was 300 μL/min, and the column was maintained at 40°C. The samples were maintained at 10°C prior to injection. The ESI voltage was set to 4,000 V, the source temperature was 350°C, and nitrogen was the nebulizing and sheath gas. Following ionization, deprotonated molecular ions ([M-H]-) were fragmented by collision-induced dissociation using nitrogen gas, then detected by multiple reaction monitoring (MRM) of fragment ions. The MRM transitions are summarized in Table 3. Quantification was performed using the internal and external standard method. Chromatograms for standards were used to calculate characteristic retention times of each compound, after which the calibration lines were applied to verify that the MS signal was linear for all analytical components over this range. Each analyte peak-area ratio to the I.S. [12(S) -HETE-d_8] was calculated and plotted against the concentration of the calibration standards, after which calibration lines were established by the least squares linear regression method [4]. Both (R)- and (S)-enantiomers of 12-HETE were calculated relative to the corresponding 12(S)-HETE-d_8.

Statistical analysis

Data are presented as the mean ± standard deviation. Statistical analyses were performed with a Student's *t*-test for the experiments with two groups. A p value < 0.05 was considered significant.

Results

Development of AD-like skin lesions

Skin dryness appeared initially after repeated application of DNCB to the dorsal shaved skin of BALB/c mice, followed by mild erythema. On day 49, the skin exhibited severe erythema, scaling and hemorrhagic crust (panel B in Fig. 1).

Histopathological changes in DNCB-induced AD mice model

A histopathological examination was performed with H&E staining of the involved skin, spleen, and lymph nodes. DNCB-treated skin revealed significant histopathological changes such as infiltration of numerous eosinophils, mononuclear cells and hyperkeratosis. Elevated mast cell numbers with mild degranulation were found under toluidine blue staining (panel C in Fig. 1).

We also found histopathological changes in the spleen and lymph nodes of the DNCB-induced AD mice model. White pulp in the spleen of the DNCB-treated mice was heterogeneous, and the number of reticular and giant cells had increased relative to those in AOO-treated mice. Mild lymphocyte depletion and granular lymphocytes were found in the lymph nodes of the DNCB-treated mice (panel C in Fig. 1).

HETE enantiomers in DNCB-induced AD mice

The chiral LC-MS/MS method achieved excellent resolution of the enantiomers of each HETE regioisomer, with typical resolution of ≥ 15 min between the (R)- and (S)- forms. The (R) enantiomer eluted at ~10 min, while the (S) enantiomer

Table 3. Multiple reaction monitoring (MRM) transitions for chiral liquid chromatography-tandem mass spectrometry analysis of 12(R)- and 12(S)-hydroxyeicosatetraenoic acid (HETE) enantiomers

Compound	[M-H]-(m/z)	MRM transition	Collision energy (eV)	Fragmentor (V)	Dwell
(±)12-HETEs	319	319 → 257 319 → 179	15	90	200
12(S)-HETE-d_8	327	327 → 264 327 → 184	15	90	200

eluted at ~13 min, and 12(S)-HETE-d_8 eluted at ~13 min (Fig. 2).

The MS/MS spectra of (±)12-HETE and 12(S)-HETE-d_8 are shown in Fig. 3. The MS/MS spectra of (±)12-HETE (m/z 319 → full scan) showed two strong signals at m/z 257 and m/z 179, suggesting that the m/z 257 signal in the spectrum of (±)12-HETE was formed by loss of water (m/z 319 → m/z 301) and CO_2 (m/z 301 → m/z 257). The signal at m/z 179 may have reflected cleavage between C-11 and C-12. Analysis of the fragmentation of the m/z 179 ion yielded a base-peak at m/z 135 (179−44).

The corresponding ions of the 12(S)-HETE-d_8 MS/MS spectrum (m/z 327 → full scan) were apparently present at m/z 264 and m/z 184 (Fig. 3). The daughter ion was formed by loss of water (m/z 327 → m/z 309) and CO_2 (m/z 309 → m/z 264). The homogenized tissues and mouse plasma homogenates were spiked with 12(S)-HETE-d_8 to determine the linearity of extraction and the analyses of eicosanoids of interest. Specifically, eight concentrations (range, 1−5,000 ng/mL) were used to create the standard curve for calibration and the R^2 value was > 0.999.

A representative LC-MS/MS spectrum and MRM analysis for the (±)12-HETEs in plasma, skin, spleen, and lymph nodes is shown in Fig. 4. These eicosanoids were identified based on their authentic standards. The biological samples (plasma, skin, spleen, and lymph node) of DNCB-treated mice had significantly increased levels of both 12(R)- and 12(S)-HETEs compared to those in AOO-treated mice, reflecting the involvement of (±)12-HETEs in AD (panels A and B in Fig. 5). The averages and changes of 12(R)- and 12(S)-HETEs values in AOO- or DNCB-treated mice (plasma, skin, spleen and lymph node) are displayed in Table 4. The LOD (limit of detection), LOQ (limit of quantitation), accuracy and precision of the LC-MS/MS analyses are displayed in Table 5.

Measurement of serum IgE levels

Serum IgE levels in the AOO and DNCB-treated groups were determined by ELISA. Total serum IgE levels increased significantly in the DNCB-treated group relative to those in the AOO-treated group. The mean serum IgE level in the DNCB-treated group was 1,931.7 ng/mL, while the mean serum IgE level in the AOO-treated group was 327.82 ng/mL (panel C in Fig. 5).

Discussion

Repeated DNCB applications induce atopic AD-like skin lesions in BALB/c mice [9,15]. In this study, AD was successfully induced by administering DNCB. This model

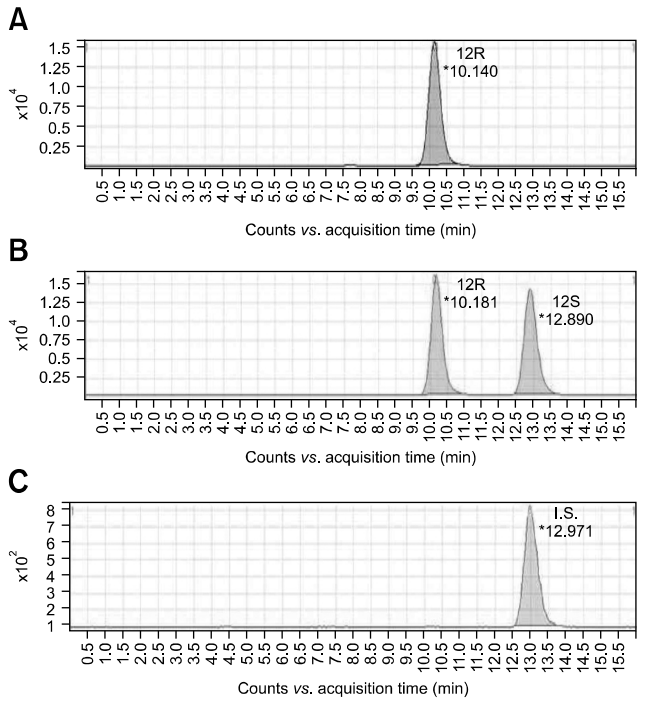

Fig. 2. Chiral separation of (±)12-HETE standards by liquid chromatography-tandem mass spectrometry analysis. 12(R)-HETE standard eluted at 10.140 min (A). Chiral separation of (±)12-HETE standards; 12(R)-HETE eluted at 10.181 min and 12(S)-HETE eluted at 12.890 min (B). 12(S)-HETE d_8 standard eluted at 12.971 min (C).

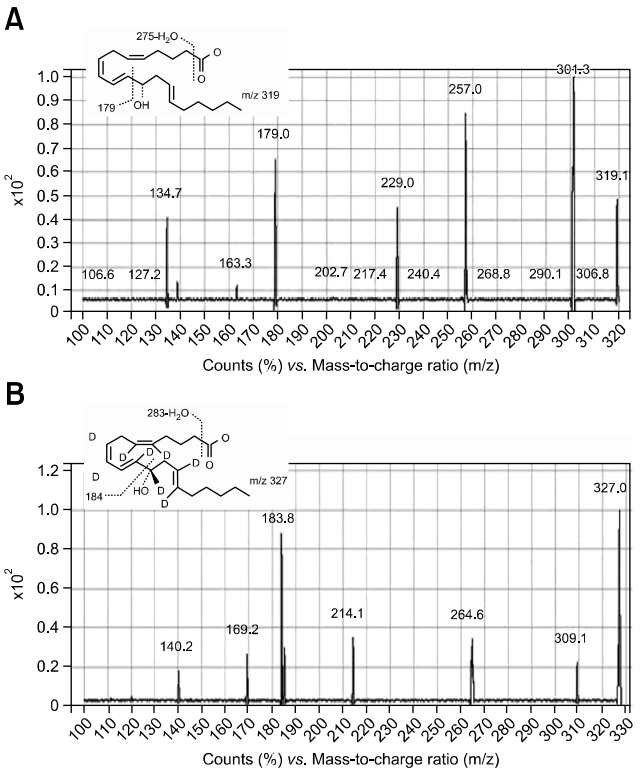

Fig. 3. Product ion mass spectra of the (A) (±)12-HETE standard and (B) internal standard (I.S.). Deprotonated molecules (m/z 319 for (±)12-HETE and m/z 327 for I.S.) were chosen as the precursor ions in the tandem mass spectrometry experiments.

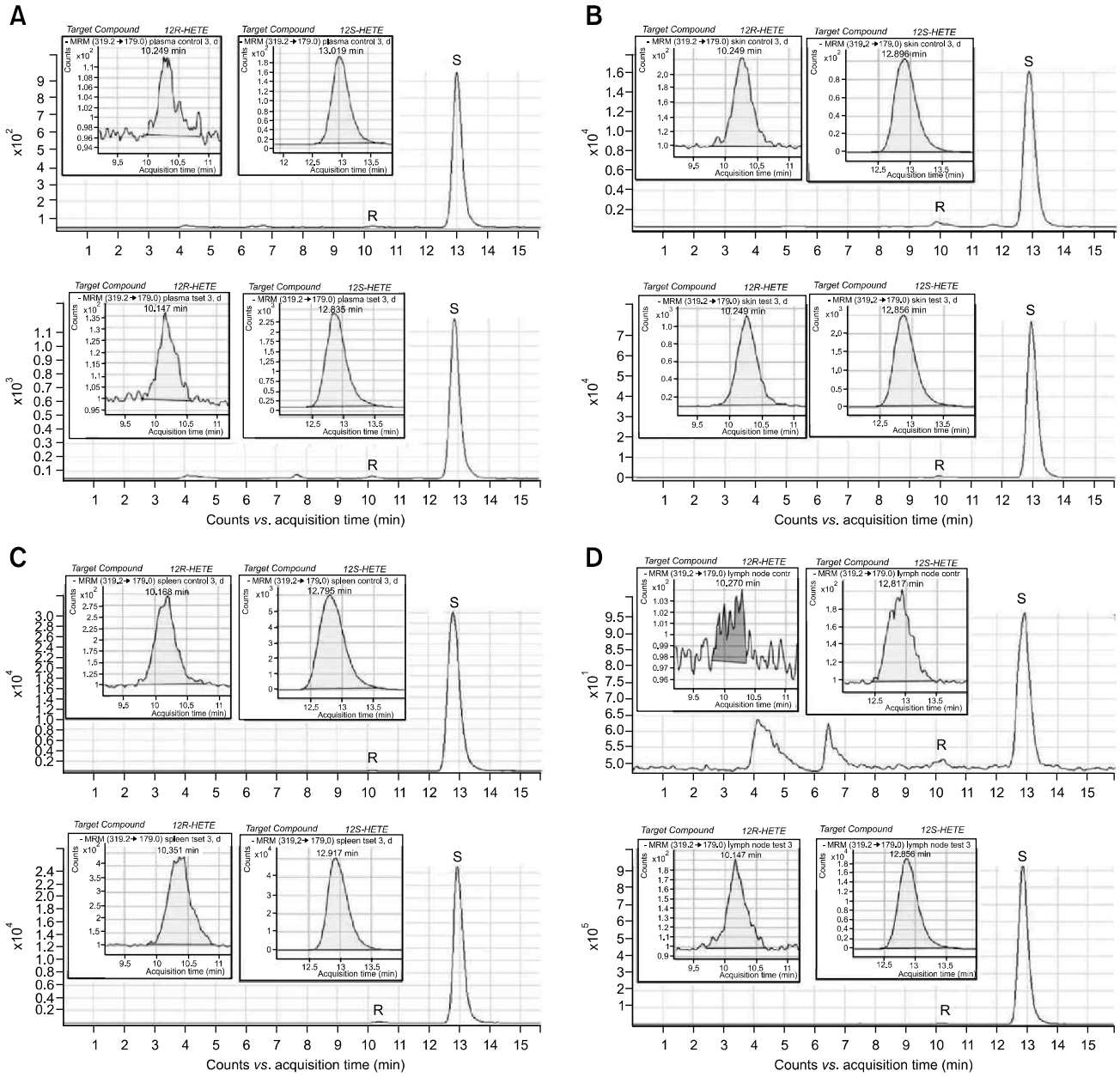

Fig. 4. Chiral LC/Ms/MS analysis and quantification of (±)12-HETE from AOO or DNCB-treated mice samples. Representative chromatograms of (±)12-HETE released from (A) plasma, (B) skin, (C) spleen, (D) lymph nodes of AOO-treated (top) and DNCB-treated mice (bottom). All (±)12-HETEs (A–D) were detected by electrospray negative ionization and multiple-reaction monitoring of the transition ions for the metabolites.

shows clinical symptoms including skin dryness, mild erythema and edema. Finally skin thickness and scaling, severe erythema and hemorrhagic were observed. Histologically, the lesioned skin showed significant thickening of the dermis and epidermis, hyperkeratosis, and parakeratosis. These symptomatic changes were relevant to an increased number of mast cells with mild degranulation and numerous eosinophils and lymphocytes infiltration in the skin lesions. Various chemical mediators and cytokines were released from activated mast cells, which might lead to primary inflammation in the skin with infiltration of eosinophils [16]. In addition, IgE levels increased significantly in DNCB-induced AD mice relative to those in AOO-treated mice. Moreover, IgE levels were associated with clinical severity of AD in DNCB treated mice, which is similar to a report for patients with AD and hyper-production of IgE [7]. Various chemotactic mediators are produced from membrane

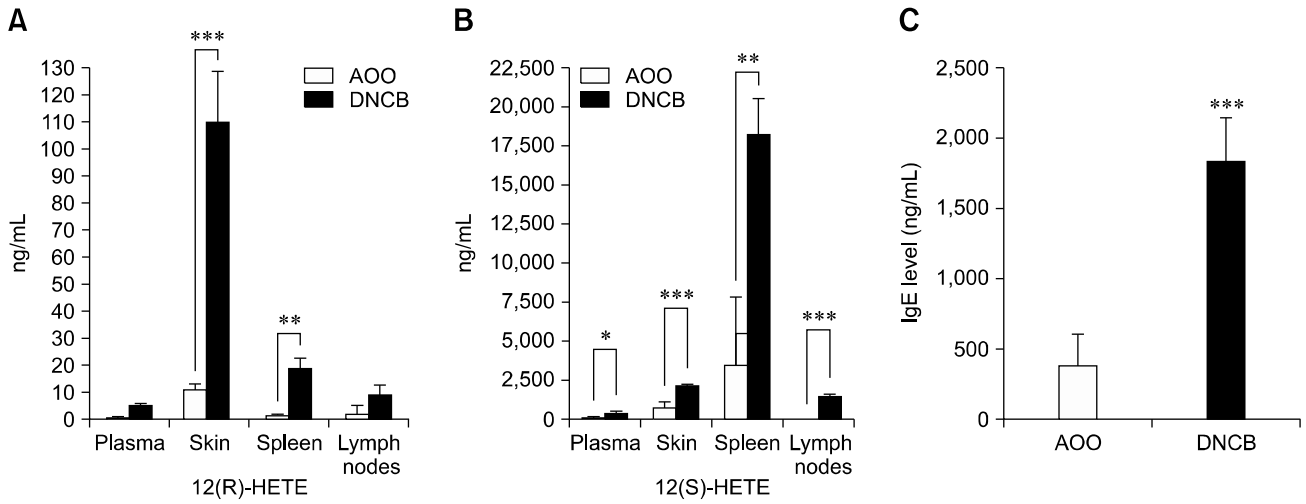

Fig. 5. (A and B) Comparison of levels of (±)12-HETE and (C) consecutive changes in total serum IgE levels (ng/mL) in AOO-treated and DNCB-treated mice. (A and B) Brackets indicate significant differences between means (*$p < 0.05$, **$p < 0.01$, ***$p < 0.001$). All results are the means ± standard deviations (SD) (n = 5). Note the different scales for 12(R)-HETE and 12(S)-HETE. (C) The mean serum IgE level of AOO-treated mice remained low (327.82 ng/mL), whereas the mean serum IgE level of DNCB-treated mice increased to a very high level (1,931.7 ng/mL). Values are the means ± SD (n = 5). ***$p < 0.001$ compared to the AOO-treated group based on a paired *t*-test.

Table 4. Comparison of 12(R)- and 12(S)-HETE average levels in AOO- and DNCB-treated mice

		AOO	DNCB	Change
12(R)-HETE (ng/mL) average of 5 samples for each of the groups	Plasma	1.28	4.56	Increase of ≈ 3.56×
	Skin	10.62	109.46	Increase of ≈ 10.31×
	Spleen	1.42	18.11	Increase of ≈ 12.84×
	Lymph node	1.03	29.91	Increase of ≈ 29.04×
12(S)-HETE (ng/mL) average of 5 samples for each of the groups	Plasma	178.27	404.94	Increase of ≈ 2.27×
	Skin	722.49	2120.66	Increase of ≈ 2.94×
	Spleen	3464.20	18110.81	Increase of ≈ 5.23×
	Lymph node	11.74	1350.79	Increase of ≈ 115.06× increase

Table 5. Limit of detection (LOD), limit of quantitation (LOQ), accuracy and precision of LC-MS/MS analysis

Compound	LOD* (ng/mL)	LOQ† (ng/mL)	Concentration (ng/mL)	Accuracy‡ (recovery %)	Precision‡ (%)
12(R)-HETE	0.0078	0.0237	10	91.7	5.9
			25	100.5	2.7
			50	101.6	3.1
12(S)-HETE	0.0084	0.0253	10	90.5	6.4
			25	100.2	2.8
			50	111.2	3.7

*3.3 σ/S (σ, standard deviation of the response; S, slope of the calibration curve). †10 σ/S. ‡Precision: % relative standard deviation (n=7 injections).

lipids following IgE-dependent stimulation of immune response. These compounds contain leukotriene B4 and various hydroxyeicosatetraenoic acids including 12-HETE [5]. In atopic dermatitis, serum IgE levels are significantly increased. Moreover, this increased IgE level can induce activation of immune response and generation of chemotactic mediators,

which leads to increased IgE and 12-HETE levels in AD. However, additional studies are needed to elucidate the relationship between IgE and HETEs in AD.

(±)12-HETEs are potent pro-inflammatory chemotactic mediators generated by epidermal keratinocytes and dermal fibroblasts. (±)12-HETE is the predominant eicosanoid significantly up-regulated in skin diseases such as AD and psoriasis [13]. AD and psoriasis are characterized by inflammation, proliferation of keratinocytes, and mast cell accumulation and activation [14]. As the spleen and lymph nodes play important roles regulating the immune system and contain a range of immune cells, we investigated the levels of (±)12-HETEs in plasma, skin, spleen, and lymph nodes of DNCB-induced AD mice by chiral LC-MS/MS. We used MRM transitions to identify individual compounds, which were confirmed by literature sources [10]. The levels of (±)12-HETEs in homogenized samples of DNCB-induced AD were significantly elevated in plasma, skin, spleen, and lymph nodes relative to those in the control group. These results show that both 12(R)-HETE and 12(S)-HETE are associated with AD pathogenesis in mice. In addition, a previous study demonstrated that the release of (±)12-HETE from platelets of AD patients was significantly higher than that in a control group [12].

Recent studies have shown that 12(R)-HETE is the up-regulated eicosanoid in psoriasis [1]. This compound is involved with 12(R)-lipoxygenase, which is associated with epidermal barrier function [6]. Our (±)12-HETE results are interesting because not only did 12(R)-HETE increase, but also 12(S)-HETE in biological samples (plasma, skin, spleen, and lymph nodes) of mice with DNCB-induced AD. These results indicate that 12(S)-HETE could be another key factor in AD pathology. In conclusion, levels of both 12(R)- and 12(S)-HETE in the plasma, skin, spleen, and lymph nodes from a DNCB-induced atopic dermatitis mouse model increased significantly. These results suggest that activation of the (±)12-lipoxygeanse pathway may play a role in AD pathogenesis.

Acknowledgments

This work was supported by the Bio-Synergy Research Project (NRF-2012M3A9C4048819) of the Ministry of Science, ICT and Future Planning through the National Research Foundation. Part of this work was also supported by the BK21 PLUS Program for Creative Veterinary Science Research. M.H. Cho was also partially supported by the Research Institute for Veterinary Science, Seoul National University, Korea.

Conflict of Interest

There is no conflict of interest.

References

1. **Bayer M, Mosandl A, Thaçi D.** Improved enantioselective analysis of polyunsaturated hydroxy fatty acids in psoriatic skin scales using high-performance liquid chromatography. J Chromatogr B Analyt Technol Biomed Life Sci 2005, **819**, 323-328.
2. **Bligh EG, Dyer WJ.** A rapid method of total lipid extraction and purification. Can J Biochem Physiol 1959, **37**, 911-917.
3. **De Benedetto A, Agnihothri R, McGirt LY, Bankova LG, Beck LA.** Atopic dermatitis: a disease caused by innate immune defects? J Invest Dermatol 2009, **129**, 14-30.
4. **de Grauw JC, van de Lest CHA, van Weeren PR.** A targeted lipidomics approach to the study of eicosanoid release in synovial joints. Arthritis Res Ther 2011, **13**, R123.
5. **Dorsh W.** Late Phase Allergic Reactions. CRC Press, Boca Raton, 1990.
6. **Epp N, Fürstenberger G, Müller K, de Juanes S, Leitges M, Hausser I, Thieme F, Liebisch G, Schmitz G, Krieg P.** 12R-lipoxygenase deficiency disrupts epidermal barrier function. J Cell Biol 2007, **177**, 173-182.
7. **Fogh K, Herlin T, Kragballe K.** Eicosanoids in skin of patients with atopic dermatitis: prostaglandin E_2 and leukotriene B_4 are present in biologically active concentrations. J Allergy Clin Immunol 1989, **83** (Pt 1), 450-455.
8. **Hammarström S, Lindgren JA, Marcelo C, Duell EA, Anderson TF, Voorhees JJ.** Arachidonic acid transformations in normal and psoriatic skin. J Invest Dermatol 1979, **73**, 180-183.
9. **Lee JK, Shin JS, Kim JH, Eom JH, Son KH, Kil JH, Kim JR, Yoon BI, Kim HS, Park KL.** Evaluation of immunosafety for skin sensitization induced by chemicals. In: National Institute of Toxicological Research (ed.). The Annual Report of Korea National Toxicology Program 2005. Vol. 4. pp. 81-90, National Institute of Toxicological Research, Seoul, 2006.
10. **Lee SH, Williams MV, DuBois RN, Blair IA.** Targeted lipidomics using electron capture atmospheric pressure chemical ionization mass spectrometry. Rapid Commun Mass Spectrom 2003, **17**, 2168-2176.
11. **McDonnell M, Davis W Jr, Li H, Funk CD.** Characterization of the murine epidermal 12/15-lipoxygenase. Prostaglandins Other Lipid Mediat 2001, **63**, 93-107.
12. **Neuber K, Hilger RA, König W.** Differential increase in 12-HETE release and CD29/CD49f expression of platelets from normal donors and from patients with atopic dermatitis by *Staphylococcus aureus*. Int Arch Allergy Immunol 1992, **98**, 339-342.
13. **Nicolaou A.** Eicosanoids in skin inflammation. Prostaglandins Leukot Essent Fatty Acids 2013, **88**, 131-138.
14. **Ozdamar SO, Seçkin D, Kandemir B, Turanli AY.** Mast cells in psoriasis. Dermatology 1996, **192**, 190.
15. **Park SJ, Lee HA, Kim JW, Lee BS, Kim EJ.** Platycodon grandiflorus alleviates DNCB-induced atopy-like dermatitis in NC/Nga mice. Indian J Pharmacol 2012, **44**, 469-474.
16. **Suto H, Matsuda H, Mitsuishi K, Hira K, Uchida T, Unno T, Ogawa H, Ra C.** NC/Nga mice: a mouse model for atopic

dermatitis. Int Arch Allergy Immunol 1999, **120** (Suppl 1), 70-75.
17. **Yamamoto M, Haruna T, Yasui K, Takahashi H, Iduhara M, Takaki S, Deguchi M, Arimura A.** A novel atopic dermatitis model induced by topical application with *Dermatophagoides farinae* extract in NC/Nga mice. Allergol Int 2007, **56**, 139-148.
18. **Yamamoto S, Suzuki H, Ueda N, Takahashi Y, Yoshimoto T.** Mammalian lipoxygenases. In: Curtis-Prior PB (ed.). The Eicosanoids. pp. 53-59, John Wiley & Sons, Chichester, 2004.
19. **Zheng Y, Yin H, Boeglin WE, Elias PM, Crumrine D, Beier DR, Brash AR.** Lipoxygenases mediate the effect of essential fatty acid in skin barrier formation: a proposed role in releasing omega-hydroxyceramide for construction of the corneocyte lipid envelope. J Biol Chem 2011, **286**, 24046-24056.